Got DRA

Laboratory for
Space Physics

Department of Physics
Washington University/St. Louis

Nuclear Interaction Tracks in Minerals and Their Implications for Extraterrestrial Materials*

G. Crozaz, M. Hair, M. Maurette,
and R. Walker
Laboratory for Space Physics
Washington University
St. Louis, Missouri 63130

*Work supported in part by NASA NAS 9-8165 and McDonnell-Douglas Contract Z80058T.

SPP-17

May, 1969

INTRODUCTION

In solid state track detectors such as mica and hypersthene crystals, only ions whose rate of primary ionization exceeds a critical value will have their path revealed as a track by an appropriate chemical etching procedure[1]. For this reason, light ions such as protons, α particles, or oxygen ions, do not directly produce tracks in mica crystals. However, when these light ions interact with heavier nuclei, the reaction products thus produced may be heavy enough to produce short interaction tracks[2,3,4].

In the present work we have studied the geometrical characteristics and the thermal stability of the interaction tracks produced by protons and α particles in mica and also in minerals which are found in meteorites or which are likely to be found in lunar materials. The energy and the fluxes of the ion were chosen to simulate exposures of $>10^3$ years in the light component of the solar flare cosmic rays. This study is the first part of a general survey which should help to predict the characteristics of the track distribution that can be expected from an exposure of meteoritic or lunar materials to solar cosmic rays.

EXPERIMENTAL TECHNIQUE AND RESULTS

Single crystals of each of the minerals were first

heated in a furnace during 8 hours at different temperatures (650°C for the muscovite samples, 800°C for the hypersthene, enstatite, diopside, hornblende crystals, 1000°C for the albite crystals), in order to anneal any fossil tracks present in the samples. Several freshly cleaved or fractured surfaces of each mineral were then heavily etched with the solution used later to reveal the interaction tracks; a background density of large etch pits, ranging from 10^3 to $10^6/cm^2$ were found on all the surfaces.

Those surfaces containing the lowest background pit densities ($< 10^4/cm^2$) were then selected and covered with thin slabs of converter materials (lexan, muscovite, Al, Zn, Au) and irradiated with protons of 11 MeV or with α particles of 30 MeV, with maximum doses of $10^{16} p/cm^2$ and $10^{15} \alpha/cm^2$. In some irradiations, the energies of the ions were changed by covering the converters with muscovite foils of different thicknesses. The reduced energies were calculated from the range energy tables of Henke and Benton[5].

After the irradiation, some of the crystals were etched directly; others were first annealed for two hours at different temperatures varying from 300°C to 900°C. The samples were all etched at room temperature as follows: 1. muscovite and hypersthene: 1 hour in HF (48%); 2. hornblende: 10 minutes in a mixture made of 2 parts HF (48%), 1 part SO_4H_2 (80%) and 4 parts of water; 3. enstatite:

2 hours in the same solution; 4. albite: 2 minutes in the same solution; 5. labradorite: 30 seconds in the same solution; 6. diopside and augite: 30 minutes in the same solution.

After the etching, we found that some of the surfaces that had been in contact with the converter foils during the irradiation were covered with small pits whose numbers greatly exceeded those of the background pits. Although these pits which we will call "interaction tracks", were observed with both an optical microscope and a stereo-scan electron microscope (figures 1 and 2), the following principal observations were made with the optical microscope:

1. The α irradiated samples of muscovite, hornblende, albite, diopside, and augite contained a measurable density of interaction tracks. The rate of production was highest in albite and lowest in augite (see Table 1). The other minerals did not show a measurable increase after irradiation.
2. The protons produced no measurable density of new pits except in the muscovite plus muscovite converter where the density of proton induced pits was lower than that produced by a flux of α particles 1000 times lower. Therefore, in the following we will speak only of α interaction tracks.
3. For the same energy of the incident α particles in the mica, the interaction track rate production,

$\Gamma_\alpha = \rho_\alpha / \Phi_\alpha$ (Φ_α is the α particle flux), is very low for the plastic converter ($\lesssim 2 \times 10^{-8}$), reaches a maximum value for the Al converter ($\sim 2 \times 10^{-7}$), and is negligible for the gold converter ($\sim 10^{-9}$).

4. Γ_α increases with the flux of α particles and decreases with a decrease in the incident energy (figure 3), (the track density also decreases with increasing annealing temperature (figure 4)).

5. The maximum depth of the etch pits observed in the muscovite and in the hornblende samples was 0.5 microns.

6. In muscovite the α interaction tracks are much less thermally stable than fission fragment tracks or α recoil tracks; the same trends are observed in hornblende for fission fragment tracks and interaction tracks (figure 4).

ORIGIN OF THE ETCH PITS

In an accelerator there is always some possibility that heavy ions, capable of registering tracks, can be present as a beam contaminant. Such particles, if present in sufficient number, could explain the observed rate of track production and the linear increase of track density with dose. However, the results of the converter experiments show clearly that such beam contaminants are <u>not</u> in fact present.

If the energy of hypothetical contaminant particles were low enough to produce tracks directly, then the density

of tracks should be highest when no converters were present. Our measurements show on the contrary that the number of tracks increases when an Al converter is placed on top of the sample. The argument is not complete however for contaminant particles of sufficiently high energy might simply be slowed down by the Al absorber to the point where they began to register tracks. This possibility can be ruled out by comparing the results obtained with different absorbing materials placed over the mica. Although the absorbing materials were adjusted to have the same total mass of material involved, neither the plastic nor the gold converters gave anywhere near the same density of tracks as the Al and mica converters.

Additional arguments can be brought to bear to show that contaminant particles are not responsible for the observed effects. As additional Al absorber is added upstream from the mica detector the rate of track production is observed to diminish as the energy of the bombarding alphas decreases. However, a measurable track production rate is observed to occur for thicknesses as great as 70 mg/cm^2.

From published data on the particle registration characteristics of mica, we estimate that neon is the lightest particle that will register a track. To penetrate the 70 mg/cm^2 of absorber where tracks are still observed to form a neon ion would have to have an energy of 15 Mev/amu. We know of no way to produce such a particle in our cyclotron.

We might finally remark that one of the original ob-

servations that led us to the study of α interaction tracks was the fact that a "spray" of short tracks could be seen on the rim of a sample of mica placed at the bottom of a cyclindral hole in an Al Target Plate. Only particles emitted from the Al side walls of the hole could have produced the observed pattern.

All the experimental results can be explained by the hypothesis that the observed tracks are produced by recoiling nuclei resulting from alpha particle interactions in the converter material. Recoils produced by either elastic or inelastic processes will go in the forward direction. In a sample that has no converter over it, only those tracks produced in the first atomic layers will intersect the surface and hence be revealed by the chemical etching*. In contrast, with a converter upstream all the particles emitted in the forward direction from the converter will cross the surface of the mica and will be revealable by etching. This explains the dramatic increase in track density when an Al converter is used.

The variation of the observed track density with different converters is also easily explained. The absence of many tracks in the case of the plastic converter is due to

*Of course if there is a general removal of surface material by the etchant this statement is no longer true. An interesting set of experiments could be performed to measure the general attack rate by detailed measurements of the alpha interaction track densities on the upstream surface following different times of attack.

the fact that none of the alpha particle reaction products are heavy enough to produce tracks in mica. The absence of many large tracks with a gold converter is explained by the large mass of the Au nucleus which prevents much energy being transferred.

The induced tracks are undoubtedly caused by recoiling nuclei resulting principally from alpha particle interactions with Si and Al. The Al converter experiments demonstrate directly that Al reaction tracks are formed, - a fact consistent with the known track registration characteristics of mica[1]. Since Si is one atomic number higher, it should also be an important track contributor.

Although it is likely that both elastic and inelastic nuclear processes are responsible for the alpha-interaction tracks, there is some evidence that the inelastic processes are dominant. In figure 3, we show the energy dependence of the track production rate in a mica + mica converter experiment. The excitation function drops steeply with decreasing energy indicating a threshold energy of 6 MeV. The fact that this is close to the Coulomb Barrier (5.6 MeV) suggests that the most of the alpha interaction tracks are produced in inelastic collisions. Measured nuclear cross-section of 1 barn for the production of alpha interaction tracks is also consistent with this view.

IMPLICATIONS FOR EXTRA-TERRESTRIAL MATERIALS

Solar cosmic rays provide an abundant source of alpha

particles of the energies that we have used here. Any sample that has been subjected to solar cosmic rays may thus be expected to contain α interaction tracks. However the penetration depth of solar cosmic rays is very small (< 1 mm); therefore, only samples that have been exposed directly to the sun's radiation, with very little intervening matter, will show these tracks.

There are at least three sources of such samples in nature: (a) materials from the surface of airless planets such as the moon; (b) interplanetary dust grains; and (c) individual meteoritic grains that were exposed to a primitive irradiation as small grains, before being incorporated into the larger meteoritic body[6,7,8].

Such samples will also contain tracks from solar wind particles* and from galactic cosmic rays. Any solar wind tracks will be extremely short (~100A°), they will be neglected in the following discussion. The galactic cosmic ray contribution has been discussed in a series of papers[11,12]. For samples at depths greater than a few mm this source of tracks will predominate. However, solar cosmic rays are much more abundant than galactic cosmic rays and provide the main source of tracks in a surface sample.

*This has not yet been verified experimentally but their existence is inferred from the observation that recoil atoms accompanying decay of U and Th gives rise to tracks[9,10]. The velocity of these particles is similar to that of the solar wind.

A mineral grain exposed to solar cosmic rays will contain two kinds of tracks: (a) a component produced by particles such as iron that are capable of registering tracks directly and (b) a component that arises from the interaction of abundant light solar cosmic rays with the constituents of the grain. In spite of their very much lower abundance, the directly registered particles initially produce many more tracks than do the interaction events. However, because heavy particles are absorbed more rapidly than light particles, the proportion of tracks that are produced by interaction events increases with increasing depth in the grain.

From calculations that will be described in more detail elsewhere, we estimate that the interaction tracks would become easily measurable at a depth of 100μ from an irradiated crystal whose sensitivity for production was equivalent to that measured here for hornblende and mica. In these calculations we took the integral energy spectrum of solar cosmic rays as $N(E) = CE^{-\alpha}$ with $\alpha = 3$[13,14]. The abundance of elements was assumed to be identical to the photospheric abundances measured in the sun.

Probably the most striking and most diagnostic effect produced by solar cosmic rays is the very rapid attenuation with depth of rather large tracks (~10μ) produced by the directly registered particles such as Fe. The importance of this effect has already been pointed out by Pellas *et al*[7] and by Lal *et al*[8]. However, the study of the interaction tracks may also

contribute much useful information. Apart from verifying the existence of a solar cosmic ray irradiation, the interaction tracks can be used to obtain additional information about the detailed irradiation history of individual grains. The track density that is observed in any grain is a function of the exposure time, the energy spectrum of solar cosmic rays, and the depth below the true surface at which the grain was irradiated. Because the variation with depth is much more rapid for the Fe tracks than for the interaction tracks, we believe that it may be possible to separate out the two parameters of exposure time and burial depth below the true surface by studying the two types of tracks. This would be particularly important in the case of lunar samples where individual grains may have suffered a complicated history as a result of "gardening" of the lunar surface. The ultimate promise of this work would be a detailed record of the past history of solar cosmic rays and hence, of the past activity of the sun.

REFERENCES

1. R. L. Fleischer, P. B. Price, R. M. Walker, E. L. Hubbard, Phys. Rev. 156, 353 (1967).
2. P. B. Price, R. M. Walker, Physics Letters 3, 113 (1962).
3. M. Maurette, R. M. Walker, Journal de Physique 25, 661 (1964).
4. P. Horn, W. Von Oertzen, Earth and Planet. Sci. Letters 2, 280 (1967).
5. R. P. Henke, E. V. Benton, USNRDL-TR-1102 (1966).
6. P. Eberhardt, J. Geiss, N. Grogler, J. Geophys. Res. 70, 4375 (1965).
7. P. Pellas, G. Poupeau, J. C. Lorin, H. Reeves, J. Audouze: (a) preprint, to be submitted to Nature (1969); (b) Trans. Am. Geophys. Union 50, 222 (1969).
8. D. Lal, R. S. Rajan, Observations Relating to Space Irradiation of Individual Crystals of Gas Rich Meteorites, preprint, to be submitted to Nature.
9. H. Huang, R. M. Walker, Science 155, 1103 (1967).
10. H. Huang, M. Maurette, R. M. Walker, Symposium on Methods of Radioactive Dating, IAEA, Monaco (1967).
11. R. L. Fleischer, P. B. Price, R. M. Walker, M. Maurette, J. Geophys. Res. 72, 331 (1967).
12. M. Maurette, P. Thro, R. M. Walker, R. Webbink, International Symposium on Meteorite Research, IAEA, Vienna (1968).
13. C. E. Fichtel, F. B. McDonald, Ann. Rev. Ast. Astrophys. 5, 351 (1967).
14. E. Stones and B. McKibben, personal communications.

FIGURE CAPTIONS

Figure 1. α interaction tracks observed in a sample of muscovite covered with a layer of muscovite, 20μ in thickness and exposed to 30 Mev α particles. Optical microscope; magnification x 1000.

Figure 2. Same α interaction tracks than in figure 1 but observed with a stereo-scan electron microscope; magnification ~6K.

Figure 3. Variation of the α interaction track rate production as a function of the energy of the α particles in samples of hornblende.

Figure 4. Annealing curve of α interaction tracks and fission fragment tracks in hornblende.

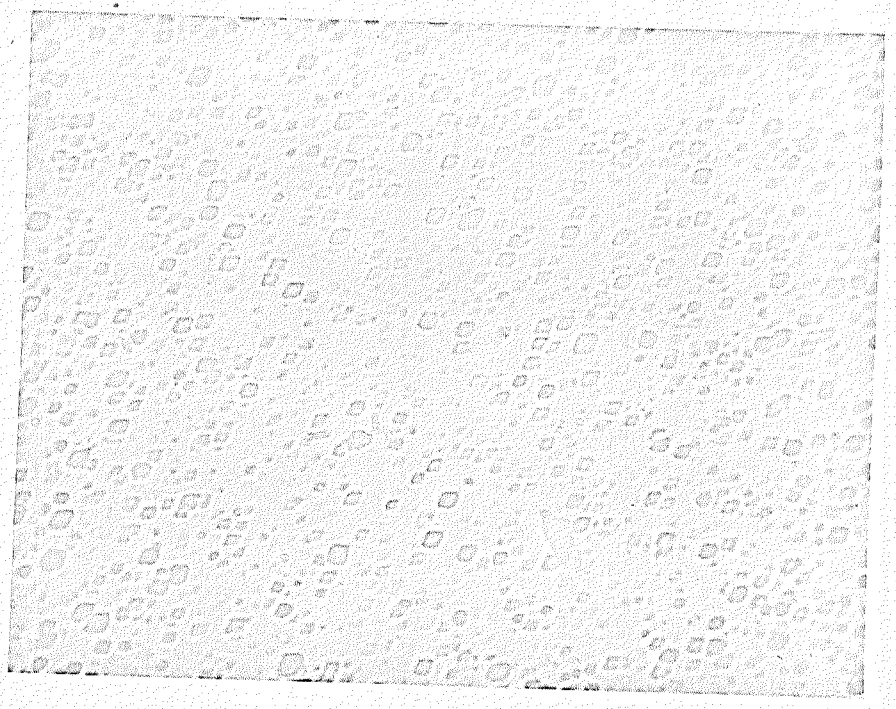

Figure 1

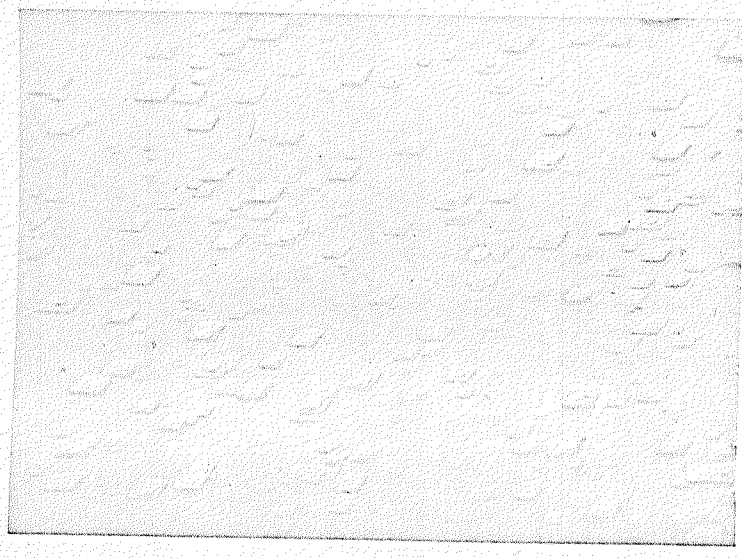

Figure 2

TABLE 1

PRODUCTION RATE OF α-INTERACTION TRACKS (MUSCOVITE CONVERTER)

Mineral	Production Rate — Optical Microscope in $nb/cm^2/\alpha$ ($\times 10^6$)	Production Rate Stereo-Scan Electron Microscope in $nb/cm^2/\alpha$ ($\times 10^6$)	Depth of the Pits (Stereo-Scan Electron Microscope) in Micron
ALBITE	3.4	4.1	≤ 0.5
MICA	0.65	1.4	≤ 0.5
HORNBLENDE			≤ 0.5
DIOPSIDE	0.26		
AUGITE	0.07		
ENSTATITE	$<10^{-3}$		
HYPERSTHENE	?		

Fig. 3